

GEOMECHANICS APPLIED TO THE PETROLEUM INDUSTRY: WELLBORE STABILITY, SAND PRODUCTION, AND HYDRAULIC FRACTURING

Nguyen Van Hung

Phenikaa University

Email: hung.nguyenvan1@phenikaa-uni.edu.vn

<https://doi.org/10.47800/PVSI.2023.02-04>

Summary

This article introduces three applications of geomechanics in oil and gas industry, encompassing wellbore stability analysis, hydraulic fracturing, and sand production. In this paper, we reviewed three commonly used applications involving transforming stress values from the in situ coordinate system to the wellbore centric coordinate system, which have been published in the previous studies. Subsequently, various failure criteria are applied to these three geomechanical problems. First, wellbore stability analysis involves six distinct scenarios across different oil reservoirs. The results obtained enable the selection of appropriate drilling mud densities to prevent collapses and instability of wellbore. Second, regarding sand production modeling, three oil fields are presented as examples. The results consistently indicate instances of sand production under various well production conditions. Finally, the application of geomechanics in hydraulic fracturing is illustrated. The findings distinctly illustrate the evolutionary pattern of fracture dimensions, highlighting a consistent trend in fracture length development. Notably, the expansion phase of the fracture exhibits a rapid onset during the initial stages, followed by a transition into an exceedingly gradual propagation state.

Key words: Geomechanics, sanding, wellbore stability analysis, hydraulic fracturing.

1. Introduction

Geomechanics plays an important role in every operation involved in the exploitation of hydrocarbon, from drilling to production and right up to the time the wells are abandoned. Reservoir pressure changes during production modify the *in situ* stresses and cause strain in both reservoir and entire sedimentary column.

One of the primary applications of geomechanics in the oil and gas sector is wellbore stability analysis [1]. As drilling operations in different geological formations, the interaction between the wellbore and formation can lead to instability issues as borehole collapse, formation damage, or fluid influx. Through geomechanical modeling and analysis, engineers can anticipate potential challenges and implement preventive measures, including mud weight, wellbore reinforcement, or casing design modifications.

Geomechanics also plays a pivotal role in hydraulic fracturing, a technique extensively used in unconvention-

al reservoirs. Assessing the stress distribution within the reservoir rock and understanding its response to hydraulic fracturing fluids is crucial in optimizing fracture design, enhancing production rates [2].

Another application of geomechanics is sand production prediction [3]. By analyzing the mechanical properties of the reservoir rock, geomechanical engineers can predict the conditions under which sand grains might detach and migrate into the wellbore. This involves studying factors such as formation strength, stress distribution, and the interaction between fluids and the rock matrix. Through geomechanical assessment, engineers can design effective sand control measures to minimize or prevent sand production. These measures may include gravel packing, sand screens, chemical consolidation, or altering production techniques to manage reservoir pressures and stresses. Moreover, ongoing geomechanical monitoring helps in identifying potential changes in reservoir conditions that might lead to increased sand production. By continuously evaluating stress changes and the mechanical behavior of the formation during production, engineers can implement proactive measures to mitigate sanding issues, thereby maintaining well integrity and productivity.



Ngày nhận bài: 6/11/2023. Ngày phân biên đánh giá và sửa chữa: 6-30/11/2023

Ngày bài báo được duyệt đăng: 7/12/2023.

The three above applications of wellbore stability analysis, hydraulic fracturing, and sand production prediction are typically presented in various studies and papers. However, these applications were presented in separate articles give rise to challenging and/or inconvenience for users to synthesize information of apply them to specific geomechanical problems. To address this issue, the author aims to integrate and introduce these three common applications of geomechanical problems in the oil and gas industry, providing engineers with a reference source for practical scenarios they might encounter. The paper presents three applied geomechanical problems as hypothetical cases applicable to diverse situations at a specified depth of the borehole. Depending on the particular situation and conditions of the boreholes, users can ascertain corresponding geomechanical parameters (e.g., via drilling log data) for application, analysis, and computation at varying depths by referencing the methodology outlined in this paper.

2. Stresses around deviated boreholes

Consider that the *in situ* principal stresses are vertical stress σ_v , major horizontal stress σ_H , and minor horizontal stress σ_h . These stresses align with the coordinate system (x', y', z') , depicted in Figure 1a. The z' -axis coincides with σ_v , x' -axis is parallel to σ_H , and y' -axis is parallel to σ_h . To analyze the stress distribution around a borehole, it is necessary to transform these original stresses into another coordinate system (x, y, z) as shown in Figure 1b. In this new coordinate system, z -axis is parallel to the borehole axis, the x -axis is parallel to the lowermost radial direction of the borehole, and the y -axis is horizontal. This transformation can be obtained by a rotation α around the z' -axis, and then a rotation i around the y' -axis (Figure 2) [4].

Using the stress transformation equation, the initial formation stresses expressed in the (x, y, z) coordinate system are transformed to:

$$\sigma_x = (\sigma_H \cos^2 \alpha + \sigma_h \sin^2 \alpha) \cos^2 i + \sigma_v \sin^2 i \quad (1a)$$

$$\sigma_y = \sigma_H \sin^2 \alpha + \sigma_h \cos^2 \alpha \quad (1b)$$

$$\sigma_z = (\sigma_H \cos^2 \alpha + \sigma_h \sin^2 \alpha) \sin^2 i + \sigma_v \cos^2 i \quad (1c)$$

$$\tau_{xy} = \frac{1}{2} (\sigma_H - \sigma_h) \sin 2\alpha \cos i \quad (1d)$$

$$\tau_{xz} = \frac{1}{2} (\sigma_H \cos^2 \alpha + \sigma_h \sin^2 \alpha - \sigma_v) \sin 2i \quad (1e)$$

$$\tau_{yz} = \frac{1}{2} (\sigma_H - \sigma_h) \sin 2\alpha \sin i \quad (1f)$$

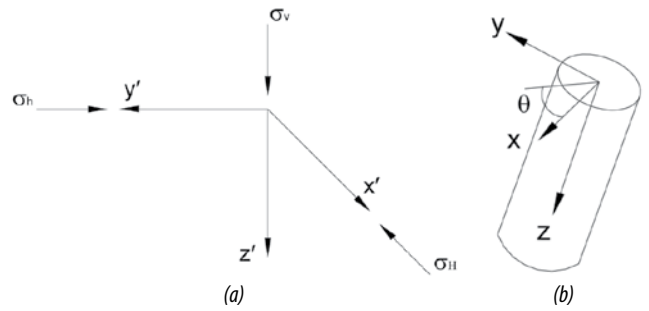


Figure 1. In situ stress co-ordinate system.

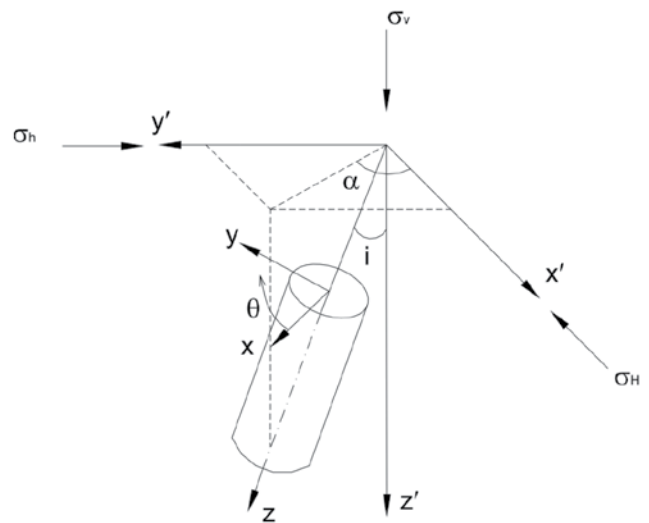


Figure 2. Stress transformation system for deviated borehole.

Nevertheless, the excavation of a wellbore will modify the *in situ* stresses that are given in the above equations. The complete stress solutions, in cylindrical co-ordinate system, around an arbitrarily oriented wellbore are:

$$\sigma_r = \frac{1}{2} (\sigma_x + \sigma_y) \left(1 - \frac{a^2}{r^2}\right) + \frac{1}{2} (\sigma_x - \sigma_y) \left(1 + 3 \frac{a^4}{r^4} - 4 \frac{a^2}{r^2}\right) \cos 2\theta + \tau_{xy} \left(1 + 3 \frac{a^4}{r^4} - 4 \frac{a^2}{r^2}\right) \sin 2\theta + \frac{a^2}{r^2} P_w \quad (2a)$$

$$\sigma_t = \frac{1}{2} (\sigma_x + \sigma_y) \left(1 + \frac{a^2}{r^2}\right) - \frac{1}{2} (\sigma_x - \sigma_y) \left(1 + 3 \frac{a^2}{r^2}\right) \cos 2\theta - \tau_{xy} \left(1 + 3 \frac{a^2}{r^2}\right) \sin 2\theta - \frac{a^2}{r^2} P_w \quad (2b)$$

$$\sigma_a = \sigma_z - 2\nu (\sigma_x - \sigma_y) \frac{a^2}{r^2} \cos 2\theta - 4\nu \tau_{xy} \frac{a^2}{r^2} \sin 2\theta \quad (2c)$$

$$\tau_{\theta z} = (\tau_{yz} \cos \theta - \tau_{xz} \sin \theta) \left(1 + \frac{a^2}{r^2}\right) \quad (2d)$$

$$\tau_{r\theta} = \left[\frac{1}{2} (\sigma_x - \sigma_y) \sin 2\theta + \tau_{xy} \cos 2\theta\right] \left(1 - 3 \frac{a^4}{r^4} + 2 \frac{a^2}{r^2}\right) \quad (2e)$$

$$\tau_{rz} = (\tau_{xy}\cos\theta + \tau_{yz}\sin\theta)(1 - \frac{a^2}{r^2}) \quad (2f)$$

$$\tau_{r\theta} = 0 \quad (5e)$$

$$\tau_{rz} = 0 \quad (5f)$$

where “a” is the radius of the wellbore, P_w is the internal wellbore pressure, and ν is a material constant called Poisson’s ratio. The angle θ is measured clockwise from x-axis as shown in Figure 2.

Deviated wellbore

For a deviated wellbore, the stress at borehole wall can be estimated by setting $r = a$ in Equation (2), which gives:

$$\sigma_r = P_w \quad (3a)$$

$$\sigma_t = (\sigma_x + \sigma_y) - 2(\sigma_x - \sigma_y)\cos2\theta - 4\tau_{xy}\sin2\theta - P_w \quad (3b)$$

$$\sigma_a = \sigma_z - 2\nu(\sigma_x - \sigma_y)\cos2\theta - 4\nu\tau_{xy}\frac{a^2}{r^2}\sin2\theta \quad (3c)$$

$$\tau_{\theta z} = (\tau_{yz}\cos\theta - \tau_{xz}\sin\theta)(1 + \frac{a^2}{r^2}) \quad (3d)$$

$$\tau_{r\theta} = [\frac{1}{2}(\sigma_x - \sigma_y)\sin2\theta + \tau_{xy}\cos2\theta](1 - 3\frac{a^4}{r^4} + 2\frac{a^2}{r^2}) \quad (3e)$$

$$\tau_{rz} = (\tau_{xy}\cos\theta + \tau_{yz}\sin\theta)(1 - \frac{a^2}{r^2}) \quad (3f)$$

Vertical wellbore

In order to determine the stresses at wall of a vertical borehole, the inclination angle I can be set to 0 in Equation (1). For simplicity, the direction $\theta = 0$ is parallel to σ_H . Consequently, the stresses become:

$$\sigma_r = P_w \quad (4a)$$

$$\sigma_t = (\sigma_H + \sigma_h) - 2(\sigma_H - \sigma_h)\cos2\theta - P_w \quad (4b)$$

$$\sigma_a = \sigma_v - 2\nu(\sigma_H - \sigma_h)\cos2\theta - P_w \quad (4c)$$

$$\tau_{\theta z} = 0 \quad (4d)$$

$$\tau_{r\theta} = 0 \quad (4e)$$

$$\tau_{rz} = 0 \quad (4f)$$

Horizontal wellbore

To estimate the stresses at the wall of a horizontal borehole, substitute $i = \pi/2$ in Equation (1). Then by introducing this into Equation (3), the stresses at borehole wall can be determined as:

$$\sigma_r = P_w \quad (5a)$$

$$\sigma_t = (\sigma_v + \sigma_H\sin^2\alpha + \sigma_h\cos^2\alpha) - 2(\sigma_v - \sigma_H\sin^2\alpha - \sigma_h\cos^2\alpha)\cos2\theta - P_w \quad (5b)$$

$$\sigma_a = \sigma_H\cos^2\alpha + \sigma_h\sin^2\alpha - 2\nu(\sigma_v - \sigma_H\sin^2\alpha - \sigma_h\cos^2\alpha)\cos2\theta - P_w \quad (5c)$$

$$\tau_{\theta z} = (\sigma_h - \sigma_H)\sin2\alpha\cos\theta \quad (5d)$$

3. Borehole stability analysis and case application

Oil fields are commonly exploited through multiple platforms that significantly impact the development costs. The use of non-vertical production wells can mitigate the need for numerous platforms. Deviated and horizontal wells substantially expand the drainage area from a single source, enhancing productivity and potentially reducing the necessity for additional platforms. In some cases, deviated boreholes are drilled to reach a substantial distance horizontally away from the drilling location. This approach efficiently accesses diverse reservoir sections, aiding in reducing the required number of platforms. Moreover, deviated boreholes serve as crucial conduits to inaccessible locations unreachable by vertical boreholes. However, drilling nonvertical boreholes introduces new challenges, including cuttings transport, casing setting and cementing, and drill string friction. An increased borehole angle will also increase the risk of borehole instability during drilling process.

Borehole instability is a significant cause of wellbore failures, presenting a critical challenge in the drilling industry. Inaccurate wellbore stability analysis leads to various issues, including borehole washouts, breakouts, collapses, pack-offs, stuck drill pipes and drill bits, and even losses of boreholes. For instance, in the Gulf of Mexico, operators encountered substantial borehole instability and sanding due to the presence of unconsolidated sands and reactive shales. The chemical impact of drilling fluid on reactive shales is another important factor affecting wellbore stability, particularly in the shales containing more smectite clay minerals. The utilization of water-based drilling mud is used, triggers chemical reactions between the shale and the mud, resulting in shale swelling and subsequent wellbore collapse. Some instances of wellbore instabilities are linked to complex geological settings, where the *in situ* stress patterns are influenced by active faults.

During the drilling phase, critical considerations involve determining the mud composition and density to maintain wellbore stability while preventing drilling fluids loss. Before full production, downhole tests encompass open-hole logging, fluid sampling, and injection tests, which may induce wellbore failure and casing collapse. As hydrocarbons are extracted and reservoir pressure gets depleted, compacting of drained formations becomes a

concern, potentially leading to solids production, casing impairment, surface subsidence, and wellbore instability. In all these stages, integrated borehole stability analyses are important to ensure reservoir production and minimize the costly problems induced by wellbore instabilities.

Wellbore stability is primarily influenced by the *in situ* stress system. During the drilling of a well, the rock surrounding the hole must take the load that was previously supported by the removed rock. Consequently, the *in situ* stresses are significantly modified near the borehole wall. This is demonstrated by the generation of increased stress around the wall of the hole, creating a stress concentration. Stress concentration can result in rock failure, particularly along the borehole wall, depending up on the existing rock strength. The fundamental challenge lies in understanding and predicting the rock behavior to the altered mechanical loading. This is a classical, though not very easy, rock mechanics problem. Typically, the possible adjustment of the borehole orientation is restricted. It is therefore obvious that wellbore instability could be prevented by mainly adjusting the mud pressure. Conventionally, the mud pressure is designed to inhibit flow of the pore fluid into the well, regardless of the rock strength and the field stresses. In practice, maintaining a minimum safe overbalance pressure, often within the range of 100 - 200 psi, or a mud density of 0.3 - 0.5 lb/gallon over the formation pore pressure, is maintained.

Stress-induced borehole failures can be categorized into three classes: hole enlargement or collapse due to brittle rock failure of the wall, hole size reduction due to ductile rock failure resulting from plastic flow of rock into the borehole, and tensile splitting of rock from excessive wellbore pressure. Selecting a failure criterion for wellbore stability analysis is challenging and confusing for drilling engineers. Determining which failure criterion should be used in the wellbore stability analysis. In fact, many failure hypotheses have been propounded as a result of theoretical reasoning only and could not be verified by experimental evidence. The Mohr-Coulomb and Drucker-Prager criterion are commonly used for wellbore stability analysis. While the Drucker-Prager criterion considers the influence of all three principal stresses on failure, the Mohr-Coulomb criterion implicitly ignores the impact of the intermediate principal stress on failure. Despite this difference, both of these failure criteria have been experimentally validated for modelling rock failure, based on conventional triaxial tests ($\sigma_1 > \sigma_2 = \sigma_3$). On the other hand, in practice, the Mohr-Coulomb crite-

riterion tends to be excessively conservative in predicting wellbore instability, whereas the Drucker-Prager criterion tends to be overly optimistic about wellbore stability. In the field, the wellbore is normally under a polyaxial stress state ($\sigma_1 > \sigma_2 > \sigma_3$), and the conventional triaxial stress state is special case that may only occasionally be encountered *in situ*. Neither the Mohr-Coulomb nor the Drucker-Prager criterion accounts for polyaxial failure mechanics. These failure criteria were established prior to the development of the first apparatus for true triaxial tests, contributing to their limited accuracy in modeling borehole failure.

Numerous authors have addressed different aspects of wellbore failure in deviated wells. Bradley [5] was the first to model compressive well failure of a deviated well, aiming to recommend appropriate mud weights to prevent borehole failure. However, his analyses were limited to the rare case where the two horizontal stresses are equal and less than the vertical stress. In a deviated well, the principal stresses acting in the vicinity of the wellbore wall are generally not aligned with the wellbore axis. To consider failure in a well of arbitrary orientation, three coordinate systems are defined. Authors always visualize wellbore failure by looking down deviated wells and assessing wellbore failure as a function of angle. Despite the complexities associated with such cases, the goal is to analyze whether the principal stresses acting in a plane tangential to the wellbore wall are such that they exceed the strength of the rock. In case of an arbitrarily deviated well, there is no simple relation between the orientation of far-field stresses and the position around the well at which either compressive or tensile failure might possibly occur. Thus, while breakouts in a vertical well always form at the azimuth of S_{hmin} , regardless of stress magnitude or rock strength (as long as the principal stresses are vertical and horizontal). This is not the case for a well that is arbitrarily oriented with respect to the *in situ* principal stresses. In this case, the position of the breakouts depends on the magnitude and orientation of principal stresses as well as the orientation of well concerning stress field.

Figure 3 illustrates the process of borehole stability analysis. The necessary input data include rock properties, earth stresses, pore pressure, and the planned trajectory of the well. For a simple analysis, only parameters listed in the first row of boxes are required. For a more advanced level of sophistication, chemical, thermal, plastic, anisotropic and time dependent features are added. In most cases, the effects are simply added by superimposing

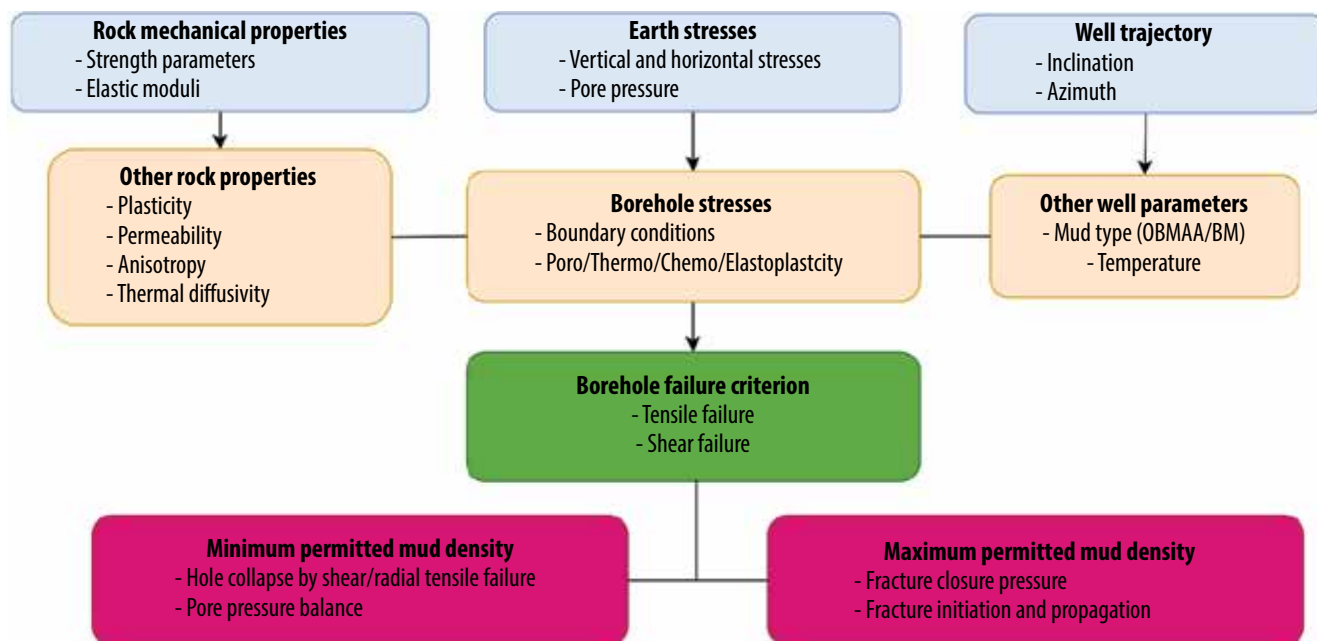


Figure 3. Flowchart showing the process sequence for wellbore design and stability analysis.

Table 1. Conditions for shear failure in vertical borehole

Case	$\sigma_1 > \sigma_2 > \sigma_3$	Borehole failure occurs at
1	$\sigma_t > \sigma_z > \sigma_r$	$P_{w,min} = P_f + \frac{2(\sigma_h - P_f) - C_0}{1 + \tan^2\beta}$
2	$\sigma_z > \sigma_t > \sigma_r$	$P_{w,min} = P_f + \frac{(\sigma_v - P_f) - C_0}{\tan^2\beta}$
3	$\sigma_z > \sigma_r > \sigma_t$	$P_{w,min} = P_f + 2(\sigma_h - P_f) - \frac{(\sigma_v - P_f) - C_0}{\tan^2\beta}$
4	$\sigma_r > \sigma_z > \sigma_t$	$P_{w,min} = P_f + \frac{2(\sigma_h - P_f)\tan^2\beta + C_0}{1 + \tan^2\beta}$
5	$\sigma_r > \sigma_t > \sigma_z$	$P_{w,min} = P_f + (\sigma_v - P_f)\tan^2\beta + C_0$
6	$\sigma_t > \sigma_r > \sigma_z$	$P_{w,min} = P_f + 2(\sigma_h - P_f) - (\sigma_v - P_f)\tan^2\beta - C_0$

*Note: In practice, cases 4, 5, 6 are only of academic interest.

poroelastic, thermoelastic and osmotic contributions to the borehole stresses. This may be satisfactory for most purposes but implies that coupling between chemical and thermal processes are neglected. The output of the analysis is the mud weight window, i.e the minimum well pressure permitted to prevent hole collapse or fluid influx and the maximum allowable well pressure permitted to prevent loss of fluid to the formation by flow into existing or induced fractures. When these limits are known, the well may be designed.

Vertical wellbore

Consider first the situation where $\sigma_t > \sigma_z > \sigma_r$ at the borehole wall. According to the Mohr-Coulomb criterion, if the well pressure drops below the value $P_{w,min}$, shear failure is expected to occur at borehole wall:

$$P_{w,min} = P_f + \frac{2(\sigma_h - P_f) - C_0}{1 + \tan^2\beta} \tag{6}$$

Next, $\sigma_z > \sigma_t > \sigma_r$, the failure criterion becomes:

$$P_{w,min} = P_f + \frac{(\sigma_v - P_f) - C_0}{\tan^2\beta} \tag{7}$$

In order to map the region of mechanical stability for a vertical well, Erling Fjar et al. [6] examined six permutations of the three principal stresses $\sigma_t, \sigma_z, \sigma_r$. The equations from this analysis are summarized in Table 1.

Based on the results of authors, cases 4, 5, 6 are mainly of academic interest. However, since they imply a wellbore pressure higher than the overburden stress, a condition that is usually unacceptable in drilling.

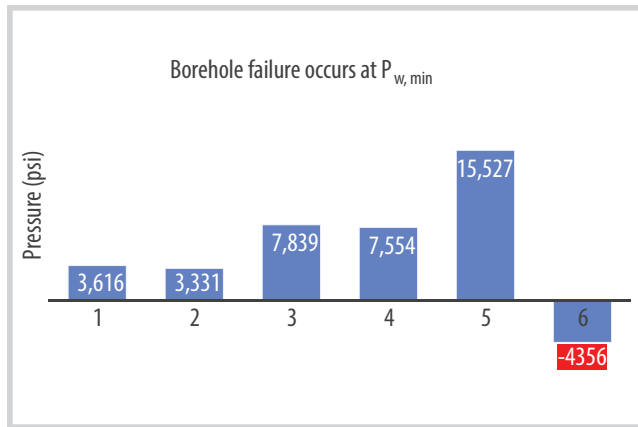


Figure 4. Minimum mud pressure of vertical well for X-field.

For a comprehensive analysis of X-field, the pay zone situated at depth of 2236.8 m, the rock reservoir had mechanical properties: $UCS = 3,744 \text{ psi}$, $\phi = 25^\circ$, $\nu = 0.2$; Earth stresses condition: $\sigma_h = 6,852 \text{ psi}$, $\sigma_H = 6,030 \text{ psi}$, $\sigma_h = 5,585 \text{ psi}$, $P_p = 3,484 \text{ psi}$.

From the findings depicted in Figure 4 across the six cases, it is evident that the maximum limiting pressure is observed in case 5. These results enable the selection of an appropriate fluid column pressure, thereby facilitating the choice of suitable drilling fluid density. Notably, in case 6, the result indicates an absence of collapse even under gas drilling conditions.

Table 2. Conditions for shear failure in horizontal borehole

$\sigma_1 > \sigma_2 > \sigma_3$	
$\sigma_t > \sigma_z > \sigma_r$	$P_{w,min} = \frac{M - UCS + P_p (\tan^2\beta - 1)}{1 + \tan^2\beta}$
$\sigma_z > \sigma_t > \sigma_r$	$P_{w,min} = \frac{\sigma_z - UCS - M \tan^2\beta + P_p (\tan^2\beta - 1)}{\tan^2\beta}$
$\sigma_z > \sigma_r > \sigma_t$	$P_{w,min} = \frac{UCS + M \tan^2\beta - \sigma_z + P_p (1 - \tan^2\beta)}{\tan^2\beta}$

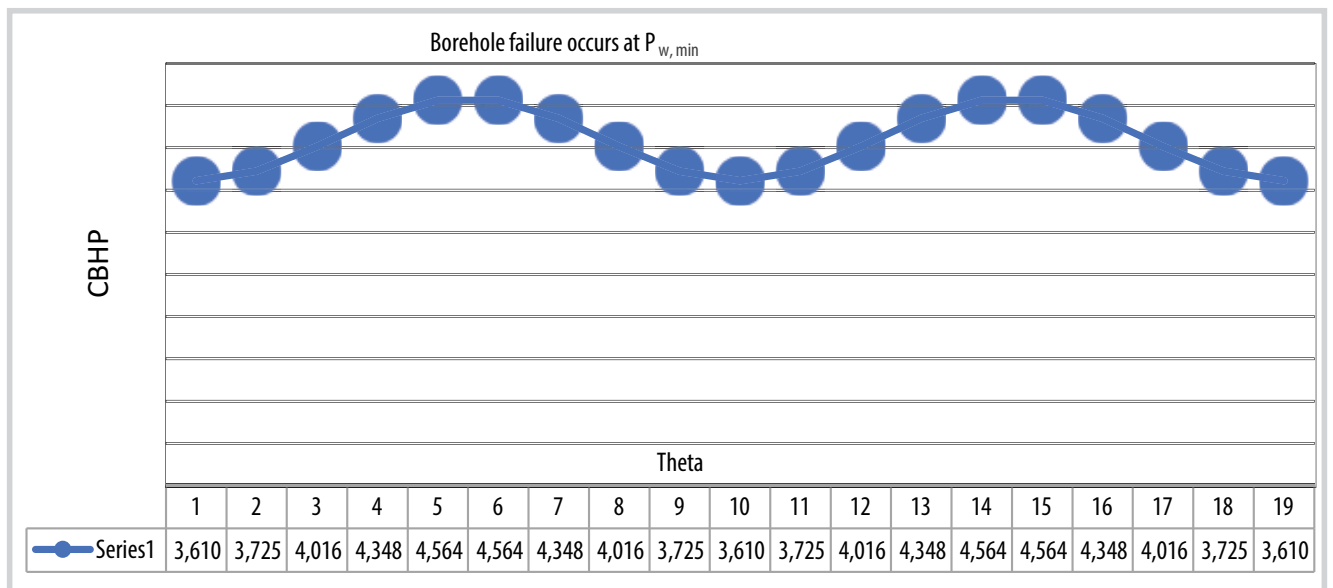


Figure 5. Minimum mud pressure of horizontal well for X-field.

Table 3. Conditions for shear failure in deviated borehole

$\sigma_1 > \sigma_2 > \sigma_3$	
$\sigma_t > \sigma_z > \sigma_r$	$P_{w,min} = \frac{\sigma_x + \sigma_y - 2(\sigma_x - \sigma_y)\cos2\theta - 4\tau_{xy}\sin2\theta - UCS + P_p (\tan^2\beta - 1)}{1 + \tan^2\beta}$
$\sigma_z > \sigma_t > \sigma_r$	$P_{w,min} = \frac{\sigma_z - UCS - M \tan^2\beta + P_p (\tan^2\beta - 1)}{\tan^2\beta}$
$\sigma_z > \sigma_r > \sigma_t$	$P_{w,min} = \frac{1}{\tan^2\beta} (UCS + (\sigma_x + \sigma_y - 2(\sigma_x - \sigma_y)\cos2\theta) - 4\tau_{xy}\sin2\theta) \tan^2\beta - \sigma_z + \nu(2(\sigma_x - \sigma_y)\cos2\theta + 4\tau_{xy}\sin2\theta) + P_p(1 - \tan^2\beta)$

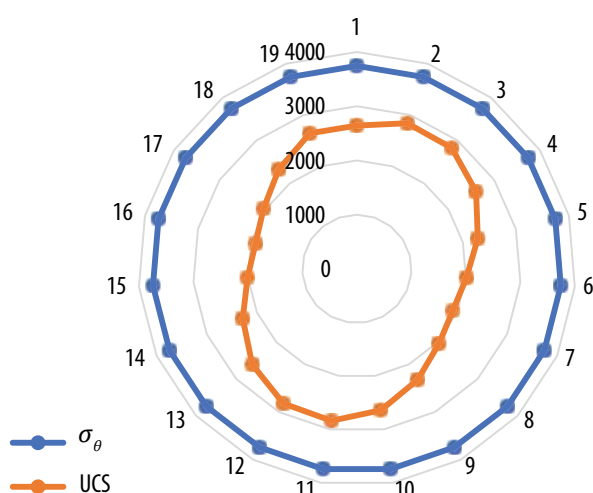


Figure 6. Stress state around the well.

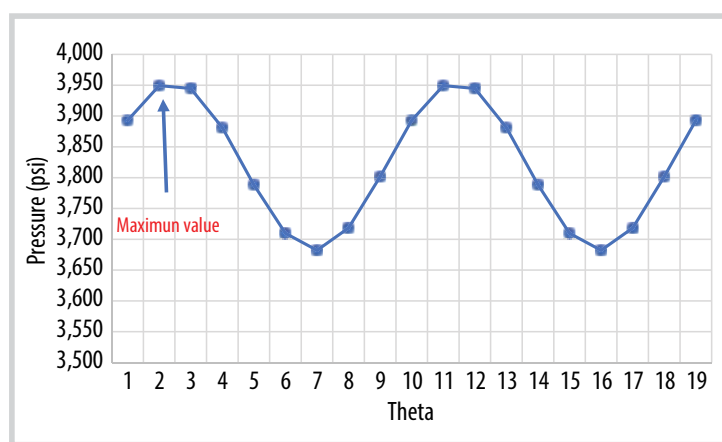


Figure 7. Minimum mud pressure of deviated well for X-field.

Horizontal wellbore

The equations for this analysis are summarized in Table 2 considering the situation where $M = (\sigma_v + \sigma_H \sin^2\alpha + \sigma_h \cos^2\alpha) - 2(\sigma_v - \sigma_H \sin^2\alpha - \sigma_h \cos^2\alpha) \cos 2\theta$.

For a comprehensive analysis of X-field, the pay zone situated at depth of 2236.8 m, the rock reservoir had mechanical properties: $UCS = 3,744 \text{ psi}$, $\phi = 25^\circ$, $\nu = 0.2$; Earth stresses condition: $\sigma_h = 6,852 \text{ psi}$, $\sigma_H = 6,030 \text{ psi}$, $\sigma_h = 5,585 \text{ psi}$, $P_p = 3,484 \text{ psi}$.

Deviated wellbore

For a comprehensive analysis of X-field, the pay zone situated at depth of 2236.8m, the rock reservoir had mechanical properties: $UCS = 3,744 \text{ psi}$, $\phi = 25^\circ$, $\nu = 0.2$; Earth stresses condition: $\sigma_h = 6,852 \text{ psi}$, $\sigma_H = 6,030 \text{ psi}$, $\sigma_h = 5,585 \text{ psi}$, $P_p = 3,484 \text{ psi}$.

4. Sand prediction and case application

Sand production refers to the movement of grains from the reservoir rock into a wellbore by the production fluid. In gas and light oil reservoirs, or offshore production, above a certain

proportion, sand production causes a number of undesirable problems such as damage to well-bore pumps and wellhead erosion, plugging of perforations or even total invasion of the production column. Numerous methods are available to tackle these issues, but their implementation tends to be costly and often results in decreased production rates. The term “solid” production is used to encompass a broader range of materials than the term “sand” which is more specific to a geological classification and grain size. In general, chalk and coal can also produce solids, ranging from sands to silts and clays. During production, stress changes around the well and the more or less constant flow of gas or oil creates instabilities which crumble the rock forming the reservoir and the fluid flow brings the material into the well. At microscopic scale, sand production is initiated when grains detach from perforations wall due to the impact of the production fluid. Particle dislodgment occurs only when the force applied to the sand particle by the fluid is greater than the sum of the shear strengths at the point of contact with the adjacent particles. It is estimated that around 70% of the world’s hydrocarbon reserves are contained in reservoirs where solid production may eventually pose a problem. The issue is particularly prominent in sand reservoirs, hence sand production has attracted the most attention.

Several factors influence solid production, but not all can be incorporated into prediction methods due to some are difficulty to recording or complexities in understanding. A first series of parameters concerns the reservoir characteristics: reservoir thickness, porosity, type, and composition of the fluid (gas, oil, water), petrophysical characteristics (rock intrinsic permeability, relative permeabilities to oil and water, oil and water viscosities, water saturation), *in situ* stress field. A second series of parameters concerns the mechanical characteristics of the reservoir rock: unconfined compressive strength, cohesion, internal angle of friction. A third series of parameters concerns well completion: well orientation and diameter, completion type (open hole, perforations), perforation characteristics, perforation radius, perforation length.

Predicting sand production aids in identifying the most cost-effective sand control methods

while maintaining the desired production rate. Once the production borehole has been drilled, cased, and cemented, the reservoir is perforated at regular intervals for production. Production begins by applying a bottomhole flowing pressure (P_{wf}) lower than the virgin reservoir pressure (P_r). The challenge arises when aiming to increase production: elevating the flowing pressure may trigger sand production, while maintaining a low flowing pressure could also induce sand production. Therefore, determining the minimum flowing pressure becomes crucial. The minimum flowing pressure in the bottomhole without sand production is the critical flowing pressure (P_{cwf}). The critical total drawdown pressure (P_{CDP}) is defined as the difference between the reservoir pressure and the critical flowing pressure. This value represents the critical drawdown from the reservoir pressure that induces failure, leading to sand production within the reservoir formation:

$$P_{CDP} = P_r - P_{cwf} \tag{8}$$

Charlez [7] examined a circular drainage area produced at a constant flow rate Q in a vertical open hole with isotropic horizontal stress ($\sigma_H = \sigma_h$). For an elastic plane stress condition and using the Mohr-Coulomb failure criterion, the critical total drawdown pressure was formulated in the following equation:

$$P_{CDP} = \frac{1}{1 - \alpha} \left[\frac{UCS}{2} - (\sigma_r - P_r) \right] \tag{9}$$

where α is Biot's effective stress coefficient.

Willson et al. [8] proposed the critical bottomhole flowing pressure resulting in sand production with assumed linear-elastic behavior.

$$P_{cwf} = \frac{3\sigma_{max} - \sigma_{min} - U}{2 - A} - P_r \frac{A}{2 - A} \tag{10}$$

where $\sigma_{max}, \sigma_{min}$ are the maximum and minimum *in situ* stresses, respectively; A is a poroelastic constant, and $A = \frac{\alpha(1-2\alpha)}{1-\alpha}$.

The critical total drawdown pressure (P_{CDP}) can be obtained:

$$P_{CDP} = \frac{1}{2 - A} [2P_r - (3\sigma_{max} - \sigma_{min} - U)] \tag{11}$$

The effective strength of the formation (U) can be obtained from the thick-walled cylinder (TWC) test, which is used as the fundamental strength measurement for unsupported boreholes and perforations:

$$U = 3.1 * TWC \tag{12}$$

where TWC is the strength as determined in the TWC test. Factor 3.1 includes the scale transformation from laboratory (OD:ID = 3) to field (OD:ID = infinity).

Based on global data on laboratory tests of the TWC and unconfined compressive strength (UCS) conducted on sandstones [9], the following correlation is presented:

$$TWC = 11.46 * UCS^{0.53} \tag{13}$$

where UCS and TWC are in MPa.

Combining Equations (12) and (13), the effective strength can be written as the following form:

$$U = 35.526 * UCS^{0.53} \tag{14}$$

Input data for three fields as below table:

Parameters	Field-1	Field-2	Field-3
Poisson ratio, ν	0.1126	0.1067	0.1717
Biot coefficient, α	0.9267	0.8689	0.7648
TWC (MPa)	12.2	30.13	103.4
σ_1 (MPa)	45.1	57	50.3
σ_3 (MPa)	38.4	51.1	44.4
P_r (MPa)	21.2	27.2	24.7

The result for three fields presented as below:

Parameters	Field-1	Field-2	Field-3
A_p	0.8091	0.7651	0.60626
U (MPa)	37.8	93.4	320.5
P_{cwf} (MPa)	35.2	4.6	-164.3

According to the results, the P_{cwf} (or CBHFP) value at Field-3 is negative. Therefore, at Field-3 there is no occurrence of sand production during the production. For Field-1, to prevent sand production, the wellbore pressure needs to be maintained at a level higher than 35.2 MPa. However, the reservoir pressure at this field is only 21.2 MPa, which is lower than the CBHFP value, so sand production will always occur under any condition of production.

5. Hydraulic fracturing and case application

Reservoir stimulation by hydraulic fracturing has become increasingly important because of its introduction in the petroleum industry in 1947. This technique is employed to stimulate reservoirs with poor or low permeability or restore some highly clogged wells and is suitable for a wide range of reservoirs (sandstone, limestone) at depths up to several kilometers. Hydraulic fracturing is commonly associated with other recovery method-

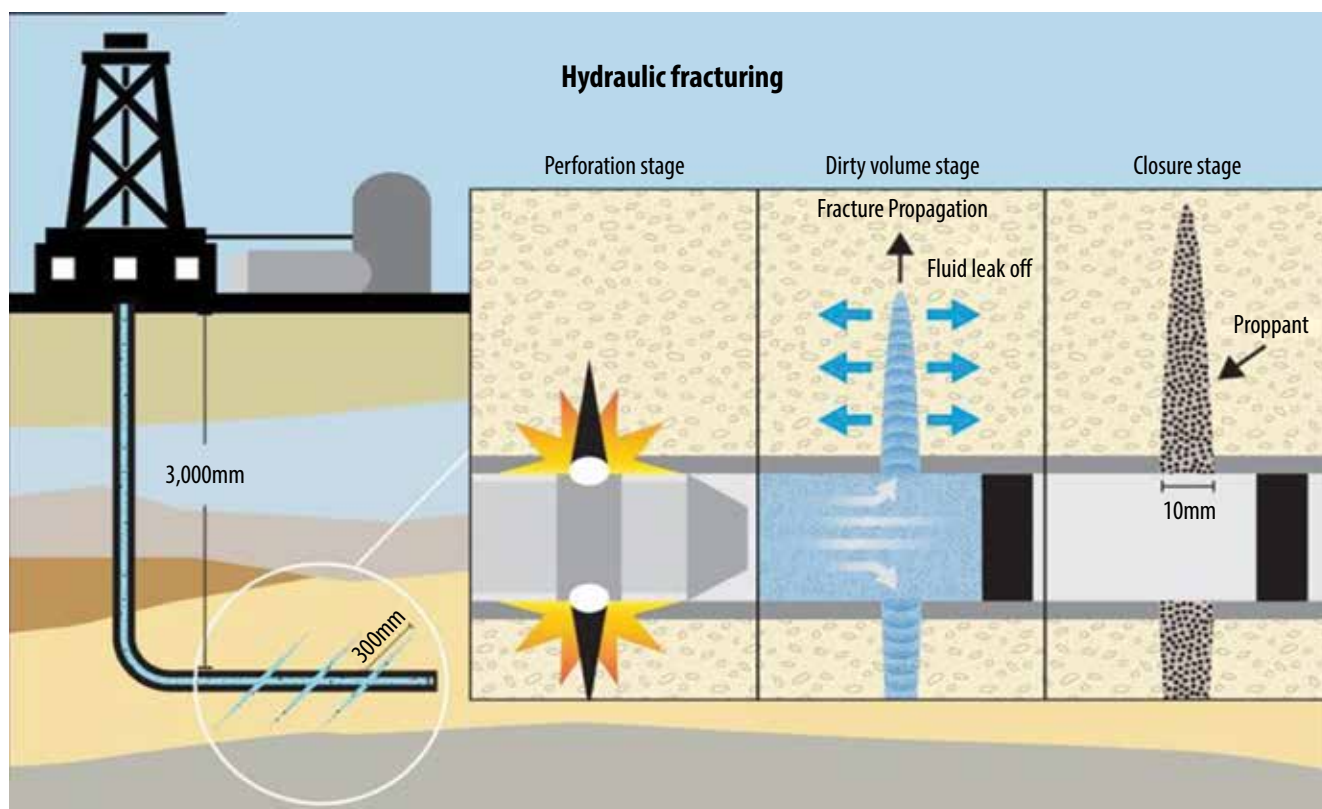


Figure 8. Schematic borehole stability analysis [11].

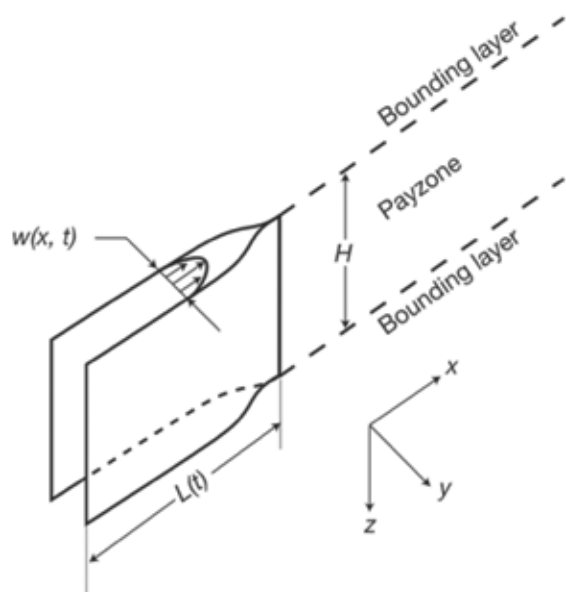


Figure 9. GDK model [13].

ologies, such as acid fracturing of carbonate formations, fracturing followed by *in situ* combustion in oil sands or oil shales.

From the viewpoint of geomechanics, the hydraulic fracturing process involves three stages (Figure 8):

- Initiation of the fracture by pressurising the medium (from the wall of the wellbore or the perforations).

- Extension of the fracture, during a granular material called a proppant in suspension in the fluid is injected, to keep the fracture open after injection.

- Removal of the fracturing fluid and recompletion of the well.

The length of the fractures ranging from 50 m to 300 m, depends on the petrophysical and mechanical properties of the treated rock. Injected volumes range from several cubic metres to several thousand cubic metres. The duration of hydraulic fracturing varies from 10 minutes to several hours. The primary challenge in designing a hydraulic fracturing operation is due to the fact that the fluid injected widens and extends the fracture but also leaks off into the formation. These two aspects must therefore be taken into consideration during the calculation. The geometry of fracture depends on the mechanical characteristics of the surrounding rock, its stress state and the fluid used.

Hydraulic fracturing modeling has been the subject of extensive research, as highlighted by Bin Chen et al., [10]. Various models have been developed to enhance the hydraulic fracturing treatment design or to understand some specific mechanisms. A series of classic hydraulic fracturing models have been developed in the period be-

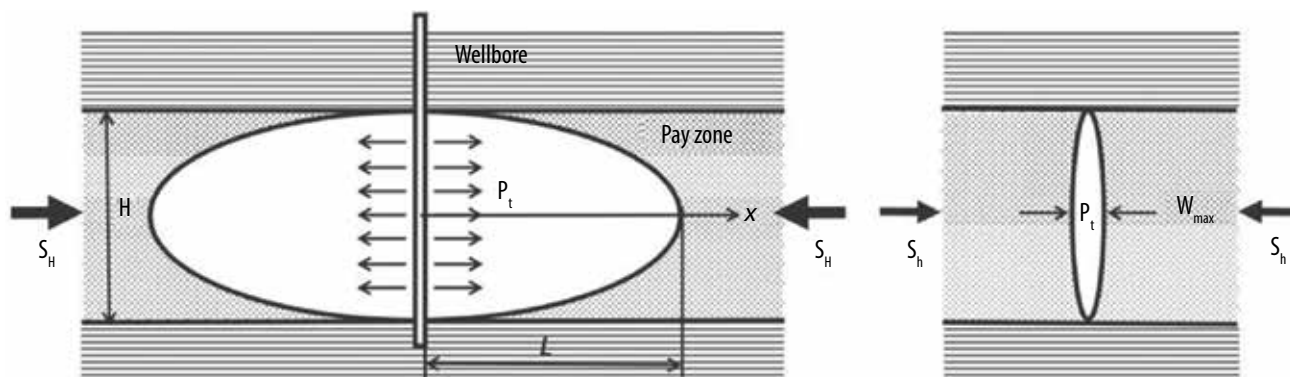


Figure 10. PKN model [13].

tween 1950s and the 1980s, such as GDK model, PKN model, the pseudo 3D (P3D) model, and the planar 3D (PL3D) model. In the following section, the author focuses on introducing the GDK and PKN models and provides real-world application examples.

GDK (Geertsma and de Klerk) type 2D models

Geertsma and de Klerk [12] presented 2D analytical solution (GDK model) for a linearly propagating fracture by assuming that the fracture height is much greater than the fracture length (height >> length). The assumptions of the GDK model are listed in the following:

- Elliptical cross section in the horizontal plane, as shown in Figure 9.
- Each horizontal plane deforms independently.
- Fracture height is a constant.
- Cross sections in the vertical plane are rectangular (fracture width is constant along its height).

The fracture width in GDK model was introduced in the following equation:

$$w^2(x) = w_0^2 \times (1 - \frac{x^2}{L^2}) \tag{15}$$

The thickness at the wellbore is given by

$$w_0 = 2.1 \left(\frac{\mu Q L^2}{Gh} \right)^{1/4} \tag{16}$$

PKN (Perkins, Kern, Nordgren) type 2D models

The model assumes that the plane strain condition is valid in each vertical plane normal to the propagation direction. It considers a con-

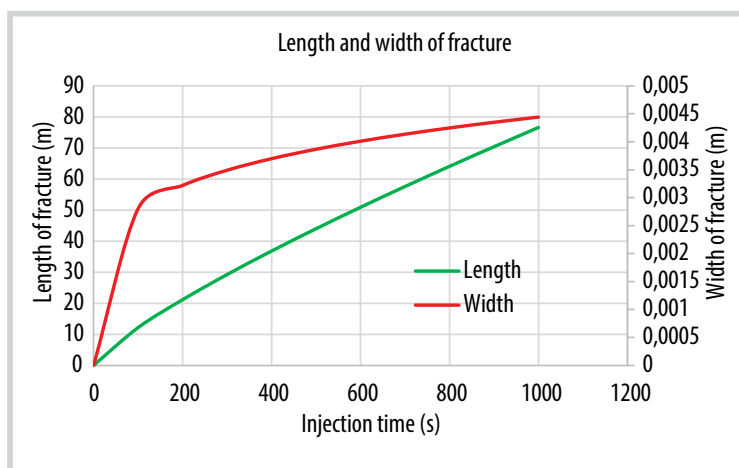


Figure 11. Fracture development using PKN model.

stant pressure vertically, diminishing with distance x and reaching zero at the fracture tip. The fracture cross-section is elliptical (Figure 10). The following analytical solutions are obtained quite simply by associating with these assumptions: 2D expression of fracture thickness, head loss in each fracture length element dL.

Without leak-off, the length and width of fracture are introduced as below:

$$L(t) = C \left[\frac{(1 - \nu)\mu Q^2}{Gh} \right]^{1/5} t^{4/5} \tag{17}$$

with C = 0.68 for 1 wing, 0.45 for 2 wings.

$$w_0(t) = \left[\frac{(1 - \nu)\mu Q^2}{Gh} \right]^{1/5} t^{1/5} \tag{18}$$

Input data as below:

Fluid viscosity, μ , MPa.s	0.00000056
Injection rate, q, m ³ /s	0.004
Poisson's ratio, ν	0.2
Shear modulus, G, MPa	10,000
Fracture height, H, m	10
Injection time, t, s	1,000

The results obtained from simulating fracture development during fluid injection using the PKN model are presented as:

The length and width of the fracture exhibit rapid development within the initial 100 seconds. After this period, the rate of width expansion slows significantly, whereas the lengthwise growth of the fracture continues. This observation aligns with empirical findings across various types of rocks.

6. Conclusions

Evaluating applications of geomechanics within the oil and gas industry introduced in this article, allowed us to conclude that employing geomechanics in wellbore stability analysis, sand production, and hydraulic fracturing plays an important role in optimizing hydrocarbon production. Some main points can be concluded through this study:

- Enabling wellbore stability analysis in the selection of appropriate drilling mud densities to prevent collapses and instability of wellbore.
- Sand production modeling consistently shows instances of sand production under diverse well production conditions.
- Width of the fracture during hydraulic fracturing process exhibits rapid onset in the first stages followed by a transition into an exceedingly gradual propagation state.

Our evaluation and reviewing of the pre-existing geomechanics analysis in hydrocarbon drilling engineering aim to assist the users in referencing suitable prediction models easily. It is noteworthy to note that modelling well stability, sand production and hydraulic fracturing is various from case to case, it depends on the input data and actual situation of each location.

References

[1] Hassan Bagheri, Abbas Ayatizadeh Tanha, Faramarz Doulati Ardejani, Mojtaba Heydari-Tajreh, and Ehsan Larki, "Geomechanical model and wellbore stability analysis utilizing acoustic impedance and reflection coefficient in a carbonate reservoir", *Journal of Petroleum Exploration and Production Technology*, Volume 11, pp. 3935 - 3961, 2021. DOI: 10.1007/s13202-021-01291-2.

[2] Zhongwei Wu, Chuanzhi Cui, Peifeng Jia, Zhen Wang, and Yingfei Sui, "Advances and challenges in

hydraulic fracturing of tight reservoir: A critical review", *Energy Geoscience*, Volume 3, Issue 4, pp. 427 - 435, 2022. DOI: 10.1016/j.engeos.2021.08.002.

[3] Nguyen Van Hung and Bui Thi Thuy Linh, "Geomechanical model and sanding onset assessment: A field case study in Vietnam", *Petrovietnam Journal*, Volume 10, pp. 40 - 46, 2021. DOI: 10.47800/PVJ.2021.10-04.

[4] Bernt S.Aadnøy and Reza Looyeh, *Petroleum rock mechanics: Drilling operations and well design, 2nd edition*. Gulf Professional Publishing, 2019.

[5] W.B. Bradley, "Failure of inclined boreholes", *Journal of Energy Resources Technology*, Volume 101, Issue 4, pp. 232 - 239, 1979. DOI: 10.1115/1.3446925.

[6] Erling Fjær, Rune Martin Holt, Per Horsrud, and Arne Marius Raaen, *Petroleum related rock mechanics, 2nd edition*. Elsevier Science, 2008.

[7] P.A.Charlez, *Rock mechanics, Volume 2: Petroleum Application*. Editions Technip, 1997.

[8] S.M.Willson, Z.A.Moschovidis, J.R.Cameron, and I.D.Palmer, "New model for prediction the rate of sand production", *SPE/ISRM Rock Mechanics Conference, Irving, Texas, 20 - 23 October 2002*. DOI: 10.2118/78168-MS.

[9] R.T.Ewy, "Wellbore stability predictions by use of a modified lade criterion", *SPE Drilling & Completion*, Volume 14, Issue 2, pp. 85 - 91, 1999. DOI: 10.2118/56862-PA.

[10] Bin Chen, Beatriz Ramos Barboza, Yanan Sun, Jie Bai, Hywel Rthomas, Martin Dutko, Mark Cottrell, and Chenfeng Li, "A review of hydraulic fracturing simulation", *Archives of Computational Methods in Engineering*, Volume 29, pp. 2113 - 2170, 2022. DOI: 10.1007/s11831-021-09653-z.

[11] Kwon Research Group, "Modeling and control of hydraulic fracturing for enhanced productivity". [Online]. Available: <https://kwon.engr.tamu.edu/research/modeling-and-control-of-hydraulic-fracturing-processes/>.

[12] J. Geertsma and F. De Klerk, "A rapid method of predicting width and extent of hydraulically induced fractures", *Journal of Petroleum Technology*, Volume 21, Issue 12, pp. 1571 - 1581, 1969. DOI: 10.2118/2458-PA.

[13] Jean-François Nauroy, *Geomechanics applied to the petroleum industry*. Editions Technip, 2011.